creative commons
COMMONS DEED

저작자표시-비영리-동일조건변경허락 2.0 대한민국

이용자는 아래의 조건을 따르는 경우에 한하여 자유롭게

- 이 저작물을 복제, 배포, 전송, 전시, 공연 및 방송할 수 있습니다.
- 이차적 저작물을 작성할 수 있습니다.

다음과 같은 조건을 따라야 합니다:

저작자표시. 귀하는 원저작자를 표시하여야 합니다.

비영리. 귀하는 이 저작물을 영리 목적으로 이용할 수 없습니다.

동일조건변경허락. 귀하가 이 저작물을 개작, 변형 또는 가공했을 경우에는, 이 저작물과 동일한 이용허락조건하에서만 배포할 수 있습니다.

- 귀하는, 이 저작물의 재이용이나 배포의 경우, 이 저작물에 적용된 이용허락조건을 명확하게 나타내어야 합니다.
- 저작권자로부터 별도의 허가를 받으면 이러한 조건들은 적용되지 않습니다.

저작권법에 따른 이용자의 권리는 위의 내용에 의하여 영향을 받지 않습니다.

이것은 이용허락규약(Legal Code)을 이해하기 쉽게 요약한 것입니다.

Disclaimer

dCollection

공학석사학위논문

다중 이동조작 로봇의 기구학적 협조제어 및 장애물 회피기법

Cooperative Grasping Control of Multiple Nonholonomic Mobile Manipulators with Obstacle Avoidance

2014 년 2 월

서울대학교 대학원

기계항공공학부

양 현 수

Abstract

Cooperative Grasping Control of Multiple Nonholonomic Mobile Manipulator with Obstacle Avoidance

Hyunsoo Yang
Mechanical & Aerospace Engineering
The Graduate School
Seoul National University

We present a novel cooperative grasping control framework for multiple kinematic nonholonomic mobile manipulators. Our control framework enables multiple mobile manipulators to drive the grasped object with velocity commands, while rigidly maintaining the grasping shape with no dedicated grasp-enforcing fixtures. And also, obstacle avoidance framework either via their whole formation maneuver or internal formation reconfiguration is proposed. For this, nonholonomic passive decomposition [1, 2] is utilized to split the robots' motion into the three aspects (i.e., grasping shape; grasped object maneuver; internal motions) so that we can control these aspects simultaneously and separately. Peculiar dynamics of the internal motions is exploited to achieve obstacle avoidance via the formation reconfiguration. Simulations are performed to support the theory.

Keywords: Nonholonomic constraint, Mobile manipulator, Obstacle avoidance, Cooperative control
Student Number: *2012-20681*

Contents

List of Figures

Abbreviations

NPD **N**onholonomic **P**assive **D**ecomposition

Symbols

$q_i \in \Re^5$	Configuration of i-th mobile manipulator
X_i, Y_i	End-effector position of i-th mobile manipuator in body frame
x_i^e, y_i^e	End-effector position of i-th mobile manipulator in inertial frame
$A_i(q_i) \in \Re^{1\times 5}$	Pfaffian constraint of i-th mobile manipulator
$h(q) \in \Re^4$	Grasping map
$\xi^h \in \Re^{15}$	Basis of shape distribution
$\xi_i^r, \xi_i^t, \xi^x, \xi^y \in \Re^{15}$	Basis of locked distribution
$\xi_i^c \in \Re^{15}$	Basis of quotient distribution

Chapter 1

Introduction

1.1 Motivation and Objectives

Robotic arms are widely used in industry and research field to perform various tasks because of its dexterous manipulation capability. Mobile robots, especially wheeled mobile robots, also allow for various applications especially those which cover wide region. From these robotic platforms, mobile manipulators [3–6] are promising for many applications, since we can combine the mobility of the mobile platform and the dexterous manipulation capability of the robotic arms attached on it. Some applications include: household assistance robots, factory automation, search and rescue, to name just few. Deploying multiple of these mobile manipulators would make more powerful applications [7, 8], by providing, e.g.,

higher manipulation dexterity, heavier payload transporting capability, and robustness against single-point failure.

When control multiple robots, cooperation is main issue to exploit advantage of multiple robots system. Cooperative grasping control is one of the important control task for multiple mobile robots control. In this thesis, we propose a novel cooperative grasping control framework for multiple kinematic planar mobile manipulators [1] under nonholonomic constraints (i.e., no-slip wheels). In particular, our control framework enables the robots to drive the grasped object under velocity commands, which embed, e.g., trajectory tracking objective, while precisely maintaining the grasping shape with no dedicated grasp/contact-enforcing fixtures and also avoiding obstacles either by changing the course of motion of their whole formation (for large obstacles) or only by reconfigurating their internal formation (for small obstacles).

For this, we utilize our recently-proposed nonholonomic passive decomposition (NPD [1, 2, 9]). Using this NPD, we can then not only split the nonholonomic systems' behaviors into the following three aspects but also control these aspects *simultaneously and separately*: 1) grasping shape control (for fixture-less rigid grasping); 2) grasped object maneuver (for the whole formation maneuver); and 3) internal motion of each mobile manipulator (for the formation reconfiguration to avoid small obstacles). Some peculiar dynamics of the internal motion of each

[1] Although the presented concepts/derivations are equally applicable to other types of mobile manipulators, for simplicity, here, we confine ourselves to a team of three planar mobile manipulators as shown in Fig. 1.1.

mobile manipulator under the combination of the control for these aspects is also exploited to achieve the obstacle avoidance strategy via internal formation reconfiguration.

Separation of control aspects, which defines our approach proposed in this thesis,, has several advantages. As mentioned in the previous paragraph, by separating each control aspect, controller for each aspect can be designed separately and their control problem can be simplified. Our decomposition-based approach can also be easily combined with previous results in autonomous control or path planning and applicable to semi-autonomous control, since, we can control each aspect simultaneously and separately. Previous path planning or tele-operation control can be applied to grasped object control which is quite straightforward. We can also achieve autonomous obstacle avoidance by simply drive the grasped object manuever, or by suitably controlling the internal motion aspect as combined with the grasped object maneuver aspect.

1.2 Relevant Works

There are a number of results, that were developed for and also relevant to the problem we consider here (e.g., [9–13]). Passive decomposition [13] was used in [10] for multiple cooperative mobile robots, yet, all the robots are holonomic. Formation control of nonholonomic mobile robots (with no manipulators on top of them) were studied in [11] (graph-based leader-follower type control reacting to

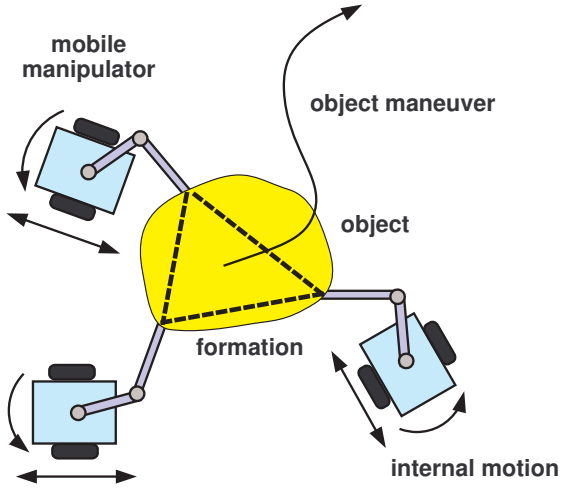

FIGURE 1.1: Three aspects of control: 1) grasping aspect; 2) grasped object maneuver; and 3) internal motion.

external obstacles), [12] (feasibility of a certain whole formation maneuver while keeping formation), and [9] (simultaneous/separate control of grasping shape and object maneuver). However, the issue of how to exploit many-DOFs of the mobile manipulators provided by their manipulating arms was not addressed there (e.g., obstacle avoidance).

Cooperative control of multiple mobile manipulators was considered in [7, 8, 14–16]. Decentralized coordination control schemes were developed in [7, 14], yet, their mobile platforms were holonomic/omni-directional (e.g., [17]) and grasp-enforcing fixtures were assumed there. Cooperation control among nonholonomic mobile manipulators was addressed in [15] using screw theory and in [8] using a

navigation function with both of them relying on the contact-enforcing fixtures. In [16], a decentralized control law was proposed, in which a novel manipulator design allows for the locomotion-manipulation control decoupling and also the fixture-less grasping. However, they did not utilize internal motion.

In contrast to these results [7, 8, 12, 14–17], our control framework presented here can: 1) take into account the nonholonomic constraints of the mobile manipulators (cf. [7, 17]); 2) rigidly maintain the grasping shape with no dedicated contact/grasp-enforcing fixtures (i.e., fixtureless grasping: cf. [7, 8, 14, 15, 17]); and 3) fully exploit the mobile manipulators' internal degree-of-freedom (DOF) to achieve, e.g., obstacle avoidance via internal formation reconfiguration without affecting the grasping and the grasped object's motion (cf. [7, 8, 14–17]).

The rest of the thesis is organized as follows. Chapter. 2 provides background materials. In Chapter. 3, using NPD [1], we split the mobile manipulators' behaviors into the three aspects as mentioned above. Chapter. 4 then presents how to achieve obstacle avoidance either via whole formation control or internal formation reconfiguration, along with some relevant simulation results. Chapter. 5 concludes the paper.

Chapter 2

System Description

2.1 System Model

In this thesis, although our proposed framework can be applied to more general cases, for simplicity, we confine ourselves to a team of three 5-DOF planar kinematic mobile manipulators as shown in Fig. 2.1(a), with the i-th robot's configuration ($i = 1, 2, 3$) given by $q_i := [x_i, y_i, \phi_i, \alpha_i, \beta_i]^T \in \Re^5$, where (x_i, y_i) is the position of the mobile platform's geometric center as measured in the inertial frame, ϕ_i is the orientation of the platform measured from the x-axis, and α_i, β_i are the relative rotation angles of the first and second links. We also denote the lengths of the two links $l_1^i, l_2^i > 0$.

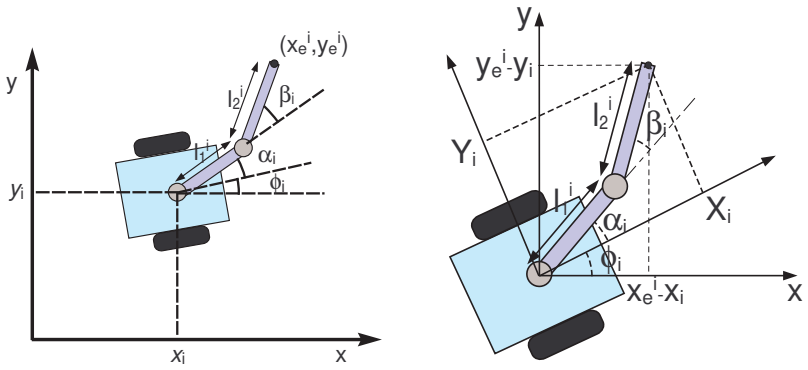

(a) (b)

FIGURE 2.1: (a) A planar mobile manipulator: (x_i, y_i) is the position of the platform center; ϕ_i, α_i, β_i are respectively the orientation of the platform and the relative angles of the first and the second links. (b) Geometry of (X_i, Y_i) and $(x_e^i - x_i, y_e^i - y_i)$.

The three mobile manipulator system in Fig. 2.1(a) is nonholonomically constrained by the following Pfaffian constraint:

$$A(q)\dot{q} = 0 \tag{2.1}$$

where $q := [q_1^T, q_2^T, q_3^T]^T \in \Re^{15}$ and

$$A(q) := \text{diag}[A_1(q_1), A_2(q_2), A_3(q_3)] \in \Re^{3\times 15}$$

with $A_i(q) \in \Re^{1\times 5}$ given by [18]

$$A_i(q_i) := \begin{bmatrix} \sin\phi_i & -\cos\phi_i & 0 & 0 & 0 \end{bmatrix}$$

encoding the no-slip wheel constraints of the platform (i.e., no side-way motion). Here, i represents index of each mobile manipulator, so that $A_i(q_i)$ is constraint for i-th robot. Under this nonholonomic constraint, the motion of the mobile manipulator is restricted to, and also can freely move in, the null-space of $A_i(q_i)$, i.e.,

$$\dot{q}_i \in \text{null}(A_i(q_i)) =: D_i(q_i)$$

where $\dim(D_i(q_i)) = 4$ which satisfy $A_i(q_i)\zeta = 0, \forall \zeta_i \in \Re^5$, s.t. $\zeta \in D_i(q_i)$. Or, equivalently, the evolution of the i-th *kinematic* mobile manipulator can be written as

$$\dot{q}_i = \begin{bmatrix} \cos\phi_i & 0 & 0 & 0 \\ \sin\phi_i & 0 & 0 & 0 \\ 0 & 1 & 0 & 0 \\ 0 & 0 & 1 & 0 \\ 0 & 0 & 0 & 1 \end{bmatrix} \begin{pmatrix} v_i \\ w_i \\ \dot{\alpha}_i \\ \dot{\beta}_i \end{pmatrix} \tag{2.2}$$

where the matrix identifies $D_i(q_i)$, v_i, w_i are the platform's linear and angular velocities, and $(\dot{\alpha}_i, \dot{\beta}_i)$ are the angular rates of each joint. Here, the control inputs for each mobile manipulator are assumed to be $(v_i, w_i, \dot{\alpha}_i, \dot{\beta}_i)$ from them being kinematic.

Therefore time derivative of the configuration of product system can be written as following

$$\dot{q} \in \text{null}(A(q)) =: D(q) \tag{2.3}$$

where $D(q)$ is the *unconstrained distribution* [19] of the nonholonomic constraint (2.1) with $\dim(D(q)) = 12$. We can also define the *constrained distribution* $D^{\perp} := \text{row}(A(q))$, any motion in which is completely suppressed by the constraint (2.1) or $A(q)\zeta \neq 0, \forall \zeta \in \Re^{15}$ s.t.,$\zeta \in D^{\perp}(q)$.

2.2 Grasping Map $h(q)$

In this thesis, we deal with cooperative grasping which is needed to be described using mathematical expression. To describe the grasping shape among the robots, following [1, 2, 9], we define the grasping map s.t.

$$h(q) := \begin{bmatrix} p_1^e - p_2^e \\ p_2^e - p_3^e \end{bmatrix} \in \Re^4 \tag{2.4}$$

where $p_i^e = [x_e^i, y_e^i]^T \in \Re^2$ is the i-th robot's end-effector position (see Fig. 2.1(a)). Note that this $h(q)$ describes the relative position vectors among the three end-effectors, with a certain value of $h(q)$ specifying a certain grasping shape among them. Also note that map $h(q)$ is not restricted to form of (2.4). Map $h(q)$ can have other form for the other control objective [1].

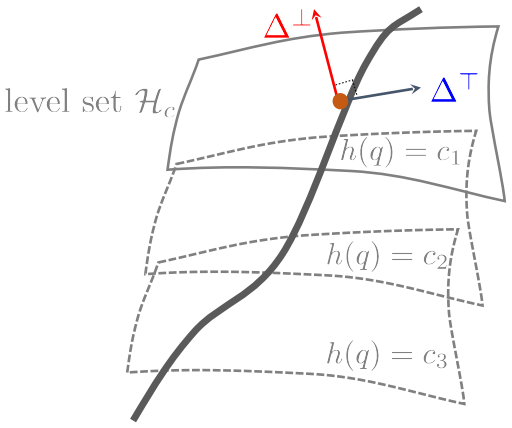

FIGURE 2.2: Geometrical representation of $\Delta^{\perp}$, $\Delta^{\top}$

From grasping map, we can consider level set of this map $\mathcal{H}_c = \{q \in \Re^{15} | h(q) = c, c \in \Re^4\}$. Then, configuration space of q can be represented as set of these level sets. And then, there are two directions at certain configuration q which are tangential to level set and normal to this direction. See Fig. 2.2. Then, similar to (2.3), we can think of the following two distributions (i.e., subset of velocity space):

$$\Delta^{\top}(q) := \{\dot{q} \in \Re^{15} | L_{\dot{q}} h(q) = 0\} = \text{null}(\partial h / \partial q) \tag{2.5}$$

$$\Delta^{\perp}(q) := \text{row}(\partial h / \partial q) \tag{2.6}$$

where $L_{\dot{q}} h(q)$ is the Lie derivative of $h(q)$ along $\dot{q}$. Here, following [1], we call $\Delta^{\top}$ the *tangential distribution*, while $\Delta^{\perp}$ the *normal distribution*. We can see that: if $\dot{q} \in \Delta^{\top}$, the grasping shape $h(q)$ will not change; if $\dot{q} \in \Delta^{\perp}(q)$, it will.

Geometrically, this normal and tangential distribution is represented as fig. 2.2. At certain configuration q, $h(q) = c_1$, $\Delta^\top$ is tangential to the level set, so that along the $\dot{q} \in \Delta^\top$ configuration will be moves in specific level set which means specific grasping shape and $\Delta^\perp$ is normal to level set, therefore along this direction configuration cannot remain certain level set.

Chapter 3

Nonholonomic Passive Decomposition

3.1 Nonholonomic passive decomposition

Given the nonholonomic constraint (2.3) and the (holonomic) grasping map $h(q)$ (2.4), utilizing the nonholonomic passive decomposition (NPD [1]), we can decompose the unconstrained distribution $D(q)$ of the multiple mobile manipulators as follows:

$$D = (D \cap \Delta^{\top}) \oplus (D \cap \Delta^{\perp}) \oplus D^{c} \tag{3.1}$$

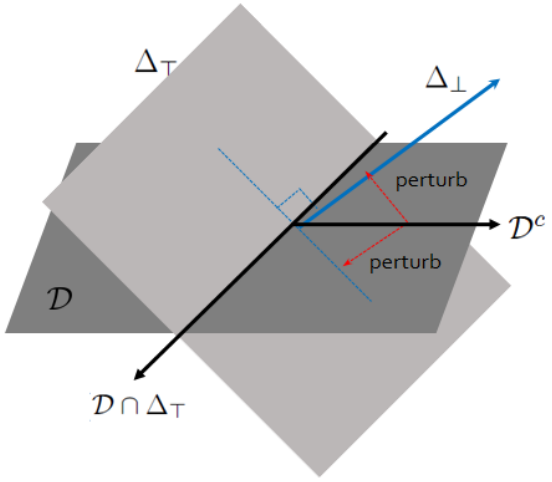

FIGURE 3.1: Geometrical representation of nonholonomic passive decomposition

where: 1) $(D \cap \Delta^\top)$ is the *locked system distribution*, specifying the directions of $\dot{q}$, which satisfy the nonholonomic constraint (2.1) while not affecting the grasping shape $h(q)$; 2) $(D \cap \Delta^\perp)$ is the *shape system distribution*, characterizing the space of $\dot{q}$, which respects the nonholonomic constraint (2.1), yet, incurs some change in the grasping shape $h(q)$; and 3) D^c is the *quotient system distribution*, any motion $\dot{q}$ in which perturbs *both* the locked and shape motions. The presence of D^c in (3.1) also means that our system is *weakly* decomposible [1].

Fig. 3.1 represent nonholonomic passive decomposition geometrically. Although dimension of system and figure is not matched, it can be shown that quotient system distribution perturb both the locked distribution and the shape distribution.

3.1.1 Shape Distribution

Following the procedure in [1], we compute each distribution of (3.1). First, we can compute the shape distribution s.t.

$$D \cap \Delta^{\perp} = \text{span}\{\xi^h\}$$

where $\xi^h(q) \in \Re^{15}$ is a (single) basis vector for $D \cap \Delta^{\perp}$, whose expression is given by

$$\xi^h = \begin{bmatrix} \xi_1^h & \xi_2^h & \xi_3^h \end{bmatrix}^T$$

where $\xi_i^h \in \Re^5$ can be written as following

$$\xi_i^h = \begin{bmatrix} c\phi_i s(\phi_j - \phi_k) \\ s\phi_i s(\phi_j - \phi_k) \\ -Y_i s(\phi_j - \phi_k) \\ -Y_i s(\phi_j - \phi_k) \\ -l_2 s(\alpha_i + \beta_i) s(\phi_j - \phi_k) \end{bmatrix}^T$$

In this expression index (i, j, k) is given as $(1, 2, 3)$, $(2, 3, 1)$, $(3, 1, 2)$ and $s(\cdot) = \sin(\cdot)$, $c(\cdot) = \cos(\cdot)$.

Here, we have $\dim(D \cap \Delta^{\perp}) = 1$, since, due to the elimination of the possible directions by the nonholonomic constraint (2.1),see fig. 3.1, we only have one direction left for changing the grasping shape $h(q)$.

3.1.2 Quotient Distribution

The quotient distribution, which is the remainder of the unconstrained distribution D with the shape and locked distributions, $\Delta^\top$ and $\Delta^\perp$, eliminated, can also be computed by

$$D^c = \text{span}\{\ \xi_1^c,\quad \xi_2^c,\quad \xi_3^c\ \}$$

with three basis vectors $\xi_i^c(q) \in \Re^{15}$. This then shows that, along this three dimensional D^c (i.e., $\dim(D^c) = 3$), the locked and the shape distributions can be perturbed at the same time. To avoid this (e.g., dropping the object with $h(q)$ being perturbed), later, we will set any control inputs in this D^c to be zero. The expression of ξ^c is too complicated, yet, not of main importance, thus, omitted here.

3.1.3 Locked Distribution

On the other hand, the locked system distribution can be obtained s.t.

$$D \cap \Delta^\top = \text{span}\{\xi^x, \xi^y, \xi_1^r, \xi_2^r, \xi_3^r, \xi_1^t, \xi_2^t, \xi_3^t\} \tag{3.2}$$

where $\xi^x, \xi^y, \xi_i^r, \xi_i^t \in \Re^{15}$ represent basis vectors (each to be explained below) with $\dim(D \cap \Delta^\top) = 8$. Recall that this locked distribution specifies the directions of $\dot{q}$, that satisfy the nonholonomic constraint (2.1) and not affect the grasping shape $h(q)$. This then implies that, if we incur some motion in this locked distribution

$D \cap \Delta^{\top}$, it will drive the mobile manipulators while leaving the grasping shape $h(q)$ intact. We will exploit this property to maneuver the grasped object and to excite some internal motion (or reconfiguration) for obstacle avoidance, while rigidly maintaining the object grasping with no dedicated fixtures.

3.1.4 Properties of Modes

For this, let us see expression of "mode" $\xi_i^r, \xi_i^t, \xi^x, \xi^y$ in (3.2). First, consider $\xi^x, \xi^y \in \Re^{15}$, whose expression are given by

$$\xi^x = \begin{bmatrix} \xi_1^x & \xi_2^x & \xi_3^x \end{bmatrix}^T, \quad \xi^y = \begin{bmatrix} \xi_1^y & \xi_2^y & \xi_3^y \end{bmatrix}^T \tag{3.3}$$

where

$$\xi_i^x := \begin{bmatrix} c\phi_i \frac{x_e^i - x_i}{X_i} & s\phi_i \frac{x_e^i - x_i}{X_i} & -s\phi_i \frac{1}{X_i} & 0 & 0 \end{bmatrix}$$
$$\xi_i^y := \begin{bmatrix} c\phi_i \frac{y_e^i - y_i}{X_i} & s\phi_i \frac{y_e^i - y_i}{X_i} & c\phi_i \frac{1}{X_i} & 0 & 0 \end{bmatrix}$$

where X_i, Y_i and $x_e^i - x_i, y_e^i - y_i$ are shown in Fig. 2.1(b). These ξ^x, ξ^y modes then respectively represent the grasped object's x and y velocity with unit speed.

As we mentioned in Chapter. 2, if we deal with more than three mobile manipulators, these vectors can also be easily obtained by just expanding the index of mobile manipulators. All of vectors only depends on its configuration. It means that the number of mobile manipulator does not affect to the expression of the

locked distribution. Therefore, although a team of three mobile manipulators is considered in this thesis, our proposed framework and derivation can be easily extended to the case of an arbitrary number of mobile manipulators.

Each modes are classified by physical behavior, so each properties will be explained At first, ξ^x, ξ^y represent unit velocity of object's x and y direction. For instance, if we drive the multiple mobile manipulators with $\dot{q} = u_x \xi^x$ with all the other modes not being excited, we have:

$$\begin{aligned} \dot{x}_e^i &= \frac{d}{dt}(x_e^i - x_i) + \dot{x}_i \\ &= \frac{d}{dt}[l_1^i \cos(\phi_i + \alpha_i) + l_2^i \cos(\phi_i + \alpha_i + \beta_i)] + \dot{x}_i \\ &= -[l_1^i \sin(\phi_i + \alpha_i) + l_2^i \sin(\phi_i + \alpha_i + \beta_i)]\dot{\phi}_i + \dot{x}_i \\ &= (y_e^i - y_i)\frac{u_x s\phi_i}{X_i} + (x_e^i - x_i)\frac{u_x c\phi_i}{X_i} = u_x \end{aligned} \tag{3.4}$$

where we use $\dot{x}_i = u_x c\phi_i (x_e^i - x_i)/X_i$ and $\dot{\phi}_i = -u_x s\phi_i / X_i$ from the definition of ξ^x, and also the geometric relations in Fig. 2.1(b) with

$$\begin{pmatrix} x_e^i - x_i \\ y_e^i - y_i \end{pmatrix} = \begin{bmatrix} c\phi_i & -s\phi_i \\ s\phi_i & c\phi_i \end{bmatrix} \begin{pmatrix} X_i \\ Y_i \end{pmatrix}$$

where this relation comes from rotational transform between inertial frame and body frame. Similarly, we can also show that $\dot{y}_e^i = u_y$ if we drive $\dot{q}$ only with

$u_y \xi^y$.

$$\begin{aligned} \dot{y}_e^i &= \frac{d}{dt}(y_e^i - y_i) + \dot{y}_i \\ &= \frac{d}{dt}[l_1^i \sin(\phi_i + \alpha_i) + l_2^i \sin(\phi_i + \alpha_i + \beta_i)] + \dot{y}_i \\ &= [l_1^i \cos(\phi_i + \alpha_i) + l_2^i \cos(\phi_i + \alpha_i + \beta_i)]\dot{\phi}_i + \dot{y}_i \\ &= (x_e^i - x_i)\frac{u_y c\phi_i}{X_i} + (y_e^i - y_i)\frac{u_y s\phi_i}{X_i} = u_y. \end{aligned} \tag{3.5}$$

This then manifests that u_x, u_y are indeed the object's x-axis and y-axis velocity, $\dot{x}_c, \dot{y}_c$, since, with $h(q)$ fixed, $\dot{x}_e^i = \dot{x}_c$ and $\dot{y}_e^i = \dot{y}_c$.

In maneuver mode ξ^x, ξ^y, there is peculiar property which is swing motion between two equilibriums. This can be shown by the expression of this modes. To show this property, we restrict translational motion to x-direction. However, following discussion can be applied to arbitrary direction because of rotational symmetry.

In the ϕ dynamics, which is given by $-\sin\phi_i/X_i$, it contains X_i term which represents x-coordinate in the body frame. And also, this dynamics have two equilibrium $\phi_i = 0, \pi$ which makes $\dot{\phi}_i = 0$. When end-effector is in front of mobile platform ($X_i > 0$), then $\phi_i = 0$ is stable equilibrium because dynamics $\dot{\phi}_i = -\sin\phi_i$ stabilize orientation to $\phi_i = 0$. However, if end-effector is in back of platform ($X_i < 0$), then *phi*-dynamics will stabilize its orientation to $\phi_i = \pi$. Using this property, system can be stabilized to each equilibrium points by changing relative position of end-effector w.r.t. mobile platform. As stated above,

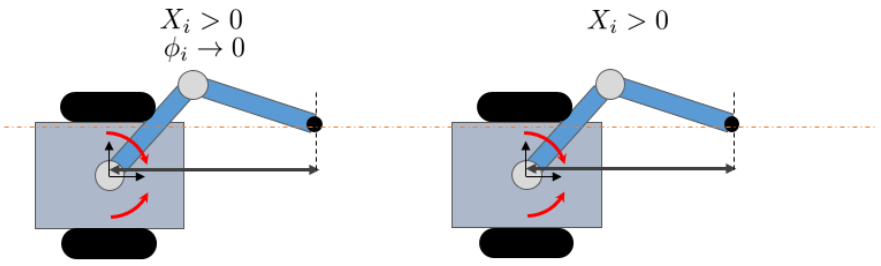

(a) When $X_i > 0$

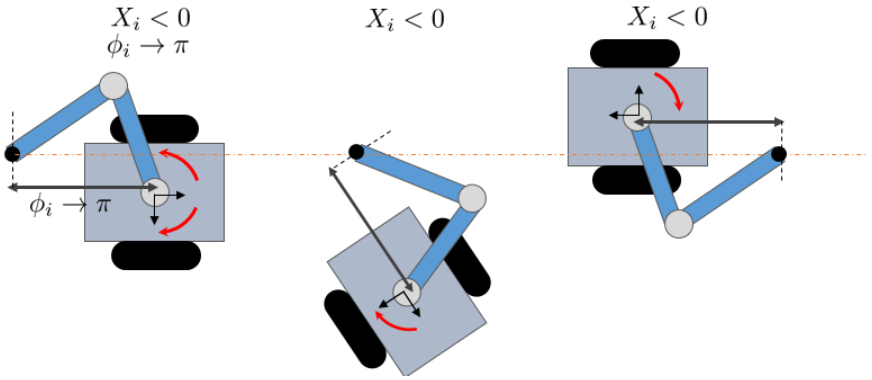

(b) When $X_i < 0$

FIGURE 3.2: Difference between (a) $X_i > 0$,(b) $X_i < 0$. When $X_i < 0$, $\phi \to \pi$ and platform rotate to put the end-effector in front of it.

relative position of end-effector can be controlled using ξ_i^t. Simulation of this "swing" motion is in Fig. 3.3.

Due to this property, end-effector tends to go in front of mobile platform. See Fig. 3.3 In the middle of the simulation in Fig. 3.3, the sign of X_i is changed

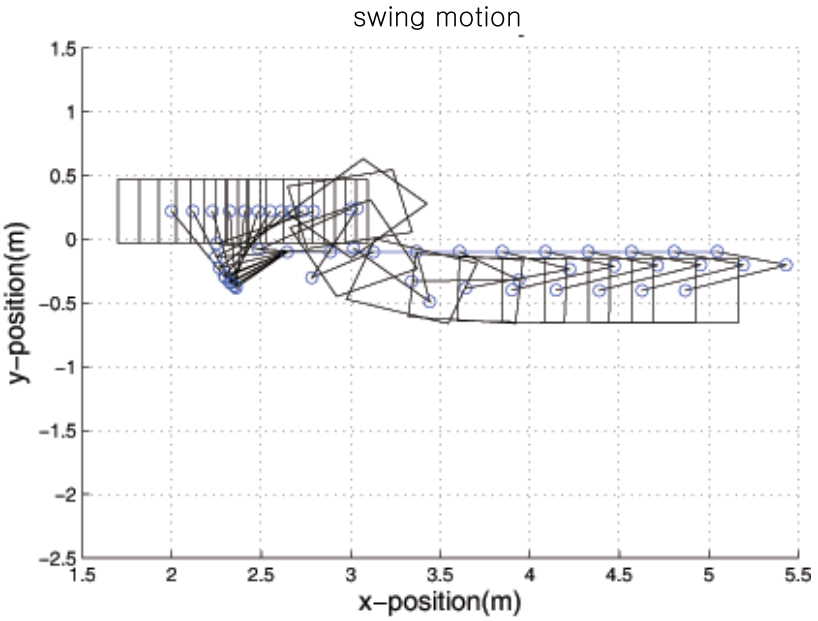

FIGURE 3.3: "swing" along x-direction

from positive to negative and it will be stabilized to $\phi_i = \pi$. As a result, end-effector goes in front of platform in inertial frame while preserving sign of X_i. This behavior is comes from internal dynamics which has some similarity with the results of [20]. This interesting "swing" motion can be exploited helpful or not. However, we can control "swing" motion by regulating X_i using other modes s.t., ξ_i^r, ξ_i^t. Fig. 3.2 shows the difference between $X_i > 0$ and $X_i < 0$, and also it shows how to change the relative position between end-effector and platform in inertial frame.

On the other hand, the modes ξ_i^r in (3.2) are given by:

$$\xi_1^r = \begin{bmatrix} 0 & 0 & 1 & -1 & 0 & 0 & \cdots & 0 \end{bmatrix}^T \in \Re^{15}$$

and ξ_2^r and ξ_3^r have a similar expression with the $(1,5)$-block of ξ_1^r shifted to $(6,10)$-block or $(11,15)$-block, while the remaining terms are all zero. Then, note that, if we drive $\dot{q}$ along this ξ_i^r, only ϕ_i and α_i of the i-th robot will rotate by the same angle, yet, in opposite direction, while keeping the posture of the two links and the end-effector position fixed. See Fig. 3.4.

Let us also consider the modes ξ_i^t in (3.2), which can be written by

$$\xi_1^t = [-l_1^1 l_2^1 c\phi_1 s\beta_1, -l_1^1 l_2^1 s\phi_1 s\beta_1, 0, l_2^1 c_{\alpha_1+\beta_1}, -X_1, 0, ..., 0]^T$$

where $c_{\alpha_1+\beta_1} = c(\alpha_1 + \beta_1)$ and ξ_2^t, ξ_3^t are also define by "shifting" this expression to the right similar for ξ_i^r as explained above. We can then show that this mode ξ_i^t represents the i-th robot as shown in Fig. 3.4, i.e., the mobile platform is translating straight back and forth with $\dot{\phi} = 0$ while leaving the end-effector position fixed (i.e., $\dot{x}_e^i = \dot{y}_e^i = 0$).

This nonholonomic passive decomposition and its associated modes then allow us to write the control equation (and the evolution $\dot{q}$) for the multiple kinematic nonholonomic mobile manipulators as follows:

$$\dot{q} = \lambda_h \xi^h + (u_x \xi^x + u_y \xi^y) + \sum_{i=1}^{3} u_i^r \xi_i^r + \sum_{i=1}^{3} u_i^t \xi_i^t + \sum_{k=1}^{3} 0 \cdot \xi_k^c \tag{3.6}$$

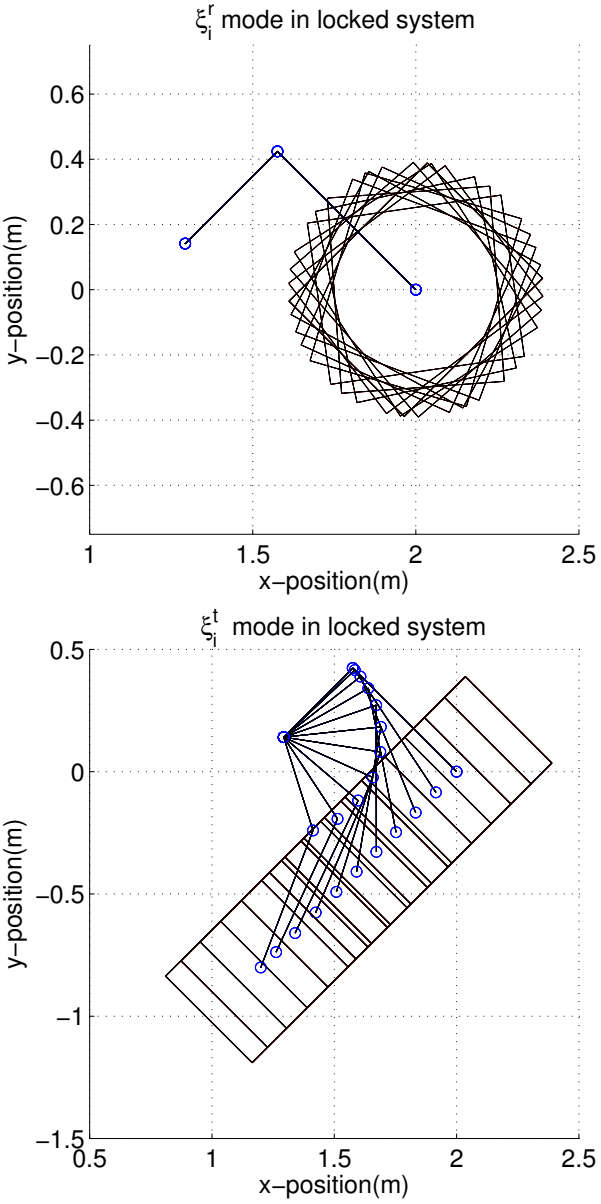

FIGURE 3.4: Motions of the modes ξ_i^r and ξ_i^t for each mobile manipulator: ξ_i^r-mode represents the rotation of the platform while keeping the end-effector position and the arm posture fixed; ξ_i^t-mode the straightline translation of the platform with the end-effector position fixed.

where $\lambda_h \in \Re$ is the grasping shape control, $u_x, u_y \in \Re$ are the grasped object's x and y maneuvering control input, and $u_i^r, u_i^t \in \Re$ are the control inputs for each robot to excite the ξ_i^r, ξ_i^t modes. Here, as stated above, we set the control input (or excitation) for the quotient distribution to be zero.

This expression (3.6) implies that we can control each mode of (3.6) simultaneously and separately, with no perturbation among them. That is, 1) by using the controls (u_x, u_y), we can drive the grasped object on the (x, y)-plane arbitrarily without affecting the cooperative grasping (i.e., $h(q)$); and 2) by using the controls (u_i^r, u_i^t), we can produce some "internal" motions for each robot while still maintaining the (fixture-less) grasping of the object and also the course of the object's motion (i.e., u_x, u_y). In the next Sec. 4, using this idea, we will design obstacle avoidance strategies for the multiple mobile manipulators by maneuvering the whole formation (and the object) via (u_x, u_y) or by reconfigurating their internal formation via u_i^r (coupled with u_x, u_y as well).

3.2 Grasping Control

Before doing so, we would like to mention the following facts about for (3.6). First, suppose that we design the grasping control λ_h s.t.

$$\lambda_h = (D \cap \Delta^\top)^T \left[\frac{\partial h}{\partial q}\right]^T \left[\frac{\partial \varphi}{\partial h}\right]^T$$

where $\varphi(h)$ is a certain potential function designed to drive $h(q) \to h_d$. Then, following [1], we can show that

$$\|h(q(t)) - h_d\| \leq \|h(q(0)) - h_d\|, \quad \forall t \geq 0$$

implying that, if we start with (fixtureless) grasping of the object by squeezing it with $h(q(0)) \approx h_d$, we can guarantee that the grasping will be maintained for all $t \geq 0$. Note also that the ξ^x, ξ^y modes in (3.3) will become singular when $X_i \to 0$, which, yet, can be avoided by using the ξ_i^t-mode.

In the next Sec. 4, we will discuss about how to combine the modes ξ^x, ξ^y, ξ_i^r to achieve the obstacle avoidance while leaving the grasping (and also the object's maneuver, if possible) intact. For this, we do not use the ξ_i^t mode, since exciting it may induce $X_i \to 0$, thereby, making ξ^x, ξ^y singular. Instead, as stated above, we sparely use this ξ_i^t-mode to mainly prevent this singularity before exciting the ξ^x, ξ^y, ξ_i^r modes.

Chapter 4

Obstacle Avoidance

4.1 Obstacle Avoidance Control Design

We consider two cases for the obstacle[1] avoidance: 1) when the obstacle is large enough so that the whole formation of the mobile manipulators and the grasped object should change its course of motion to avoid it (Fig. 4.1(a) and Fig. 4.1(b)); or 2) when the obstacle is small enough so that the mobile manipulators can avoid it by using the internal motions (e.g., formation reconfiguration) without changing the commanded trajectory of the object (Fig. 4.1(c)). During both cases for the obstacle avoidance, the grasping is maintained with no perturbation

[1]Here, we assume that the height of the obstacles are lower than the grasped object and the robot arms of each mobile manipulators (e.g., elevated mobile platforms), that is, the obstacles may be thought of as "holes" on the ground.

from the avoidance action whatsoever. For simplicity, here, we only consider the scenario where the grasped object moves along the x-axis. Note however that, due to the rotational symmetry, our results are also equally applicable when the grasped object moves along other directions.

4.1.1 Obstacle Avoidance via Whole Formation Control

Let us consider the case where the obstacle is so large that the whole formation of the robots must change its course of motion to avoid it. For this case, only utilizing the (ξ^x, ξ^y)-modes, we present two ways to achieve the obstacle avoidance: 1) whole formation control via artificial potential filed; and 2) whole formation maneuvering to pass by the obstacle. Reconfiguration-based obstacle avoidance by using the internal motion for a small obstacle will be discussed in 4.1.2. Here, we present whole formation manuever strategy for obstacle avoidance utilizing only ξ^x, ξ^y-modes with artificial potential technique. For simplicity, we assume that $u := [u_x, u_y]^T = [1, 0]^T$ (i.e., driving the object along the x-axis), although the obtained results are also valid for motions along other directions due to the system's rotational symmetry as mentioned before.

First, let us define an artificial potential function $\psi(p_c, p_o) \geq 0$, where $p_c = [x_c, y_c]^T \in \Re^2$ is the center position of the grasped object and p_o is the location of the obstacle. We design this ψ s.t.: 1) it is smooth; 2) it gets large when $|p_c - p_o|$ becomes small; and 3) its action $\frac{\partial \psi}{\partial p_c}$ gets large when $\psi(p_c, p_o)$ itself

becomes large. We then modify the command for the (ξ^x, ξ^y)-modes s.t.

$$u_v := u - \frac{\partial \psi^T}{\partial p_c} \tag{4.1}$$

where $u = [1, 0]^T$ (i.e., intended behavior is the x-axis translation), and $\frac{\partial \psi}{\partial p_c} \in \Re^{1\times 2}$ is the one-form of ψ. We can then show that

$$\begin{aligned} \frac{d\psi}{dt} &= \frac{\partial \psi}{\partial p_c}\dot{p}_c = \frac{\partial \psi}{\partial p_c}(-\frac{\partial \psi^T}{\partial p_c} + u) \\ &\leq -\|\frac{\partial \psi}{\partial p_c}\|^2 + \|\frac{\partial \psi}{\partial p_c}\| \cdot \|u\| \end{aligned}$$

where $||u|| = 1$. Now, suppose that: 1) $\exists$ a large enough $\bar{M} > 0$ such that $\psi \leq \bar{M}$ ensures no collision with the obstacle; and 2) if $\psi \geq \bar{M}$, $\|\frac{\partial \psi}{\partial p_c}\| \geq \|u\|$. Then, from the above inequality, we have $\dot{\psi} \leq 0$ whenever $\psi \geq \bar{M}$, implying that $\psi \leq \bar{M}$ $\forall t \geq 0$ (i.e., obstacle avoidance is guaranteed).

Fig. 4.1(a) presents snapshots of the simulation of this potential field method. Note that the whole formation (and the grasped object) change their course of motion to avoid the obstacle, while rigidly maintaining (fixture-less) grasping of the object. The x-velocity also deviates from the desired one (i.e., denser intervals between snapshots), due to the effect of the potential field ψ in the control u. (4.1)

Consider also the case of obstacle avoidance via whole formation maneuvering. For this, we define the desired y-position of the grasped object, y_c^d, so that the whole formation can pass by the obstacle while still moving along the x-axis with

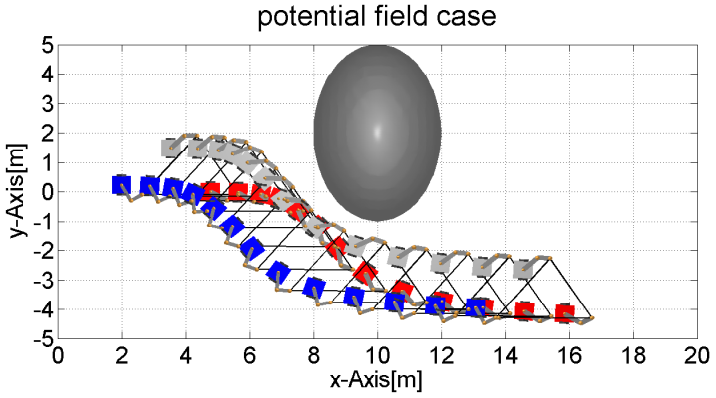

(a) Whole formation potential field

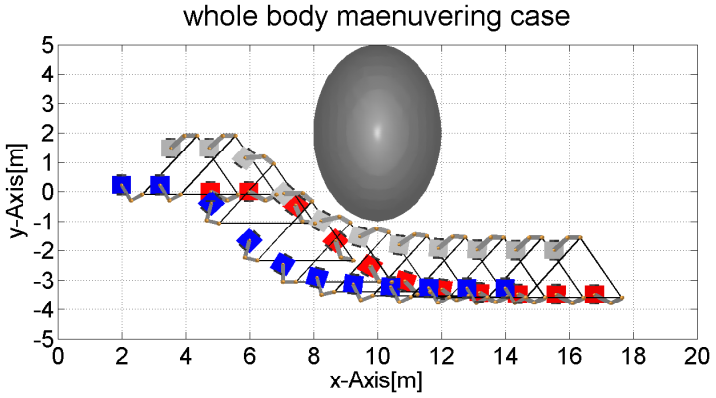

(b) Whole formation maneuvering

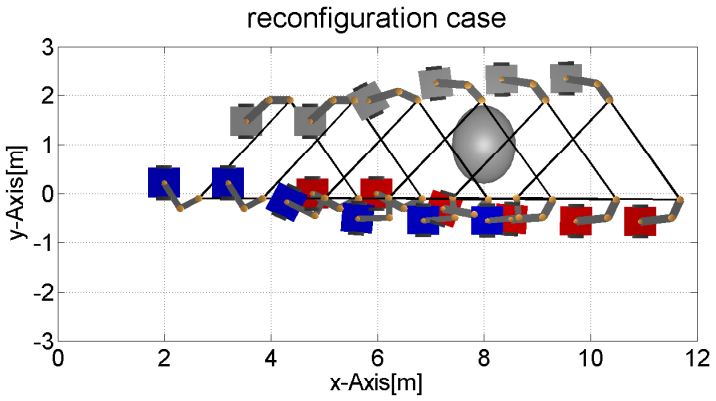

(c) Reconfiguration via internal motion

FIGURE 4.1: Snapshots of the cooperative grasping with obstacle avoidance and rigid grasp-shape keeping: 1) whole-formation potential field (top); and 2) internal motion based formation reconfiguration (bottom).

$u_x = 1$. We then design the control input u s.t.,

$$u := \begin{pmatrix} u_x \\ u_y \end{pmatrix} = \begin{pmatrix} 1 \\ -k(y_c - y_c^d) \end{pmatrix}$$

where $y_c \in \Re$ is the y-position of the grasped object's center and $k > 0$ is the control gain. Then, since u_y is the object's y-axis velocity with $h(q)$ fixed (i.e., $u_y = \dot{y}_e^i$): see Sec. 3.1, we have $y_c - y_c^d \to 0$. Thus, if we set the gain k large enough, we can make the multiple mobile manipulators to avoid the obstacle by moving up/down along the y-axis while still keeping the x-axis translation with the velocity $u_x = 1$ (i.e., uniform interval along x-axis) and also maintaining the grasping shape rigidly.

4.1.2 Obstacle Avoidance via Internal Motion

Here, we also assume for simplicity $(u_x, u_y) = (1, 0)$ and with $\phi_i(T_0) = 0$ where T_0 is initial time, while avoiding the obstacle by reconfigurating the formation via the internal motion modes ξ_i^r. Using (3.3) with $(u_x, u_y) = (1, 0)$, we can show that the dynamics of ϕ_i is given by:

$$\dot{\phi}_i = -\frac{1}{X_i} \sin \phi_i \tag{4.2}$$

where X_i is depicted in Fig. 2.1(b) with $X_i \neq 0$ if $X_i(T_0) \neq 0$ (to be enforced by our control below). This ϕ_i-dynamics (4.2) has two equilibria, $\phi_i = 0$ or $\phi_i = \pi$. Moreover, when $X_i > 0$, $\phi_i = 0$ is the stable equilibrium and $\phi_i = \pi$ is unstable

one; whereas, if $X_i < 0$, this stability property of the two equilibria are swapped with each other.

Then, we design the avoidance strategy as shown in Fig. 4.2: 1) we first define the desired configuration Y_i^d to avoid the obstacle; 2) with $u_x = 1$, we inject some feedback control u_i^r to excite the ξ_i^r-mode to achieve $Y_i \to Y_i^d$; and 3) once the desired configuration is achieved, we set $u_i^r = 0$ so that $\phi_i \to 0$ due to the stabilization of ϕ_i (with $X_i > 0$) as shown in (4.2). Note that, during this avoidance sequence, the intended object trajectory will be preserved due to vector-space split in (3.6). We also assume that there is an algorithm available to determine if the obstacle is small enough so that the avoidance strategy of Fig. 4.2 can be used and, if so, what should be Y_i^d for that.

Now, for achieving $Y_i \to Y_i^d$ via u_i^r, we utilize the following dynamics:

$$\dot{X}_i = Y_i u_i^r, \quad \dot{Y}_i = -X_i u_i^r \tag{4.3}$$

which can be obtained by using the expressions of X_i, Y_i from Fig. 2.1(b) with $\dot{\alpha}_i = -u_i^r$ and $\dot{\beta}_i = 0$ under the control u_i^r. Also, since $\dot{\beta}_i = 0$, we have

$$X_i^2 + Y_i^2 = R_i^2, \quad \forall t \geq 0$$

where $R_i^2 = l_1^{i2} + l_2^{i2} + 2l_1^i l_2^i \cos\beta_i$ is a constant with β_i fixed (see Fig. 2.1(b)). This then implies that we can think of (X_i, Y_i) as a point on the circle with the

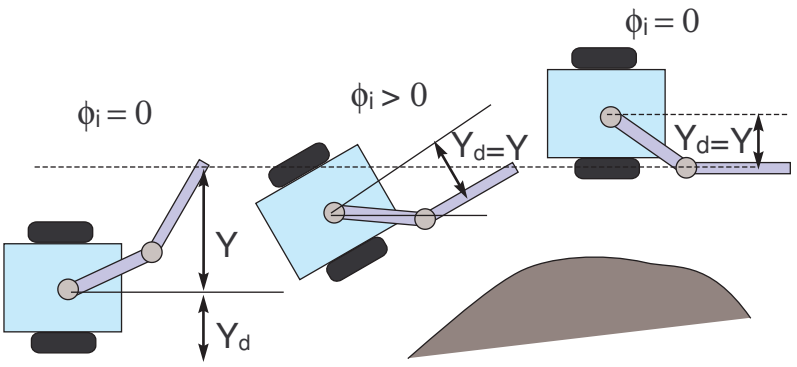

FIGURE 4.2: Obstacle avoidance strategy via internal motion: 1) initial condition with $\phi_i(0) = 0$ and the target Y_i^d computed; 2) reconfiguration with $Y_i \to Y_i^d$; and 3) stabilization with $\phi_i \to 0$.

radius $R_i > 0$, which may rotate clockwise or counterclockwise depending on the sign of u_i^r in (4.3). See Fig. 4.3.

On the circle in Fig. 4.3, we may also denote the desired configuration Y_i^d in Fig. 4.2 by (X_i^d, Y_i^d), where $|Y_i^d| < R_i$ and $X_i^d := \sqrt{R_i^2 - Y_i^{d2}}$ so as to ensure that $X_i > 0 \, \forall t \geq T_0$ to avoid the singularity in u_x (3.3). We may then achieve $Y_i \to Y_i^d$ without invoking the singularity of $X_i = 0$ by driving (X_i, Y_i) to (X_i^d, Y_i^d) while remaining in the first and fourth quadrants of Fig. 4.3. This in fact can be granted by the following feedback control:

$$u_i^r = \gamma(Y_i - Y_i^d) \tag{4.4}$$

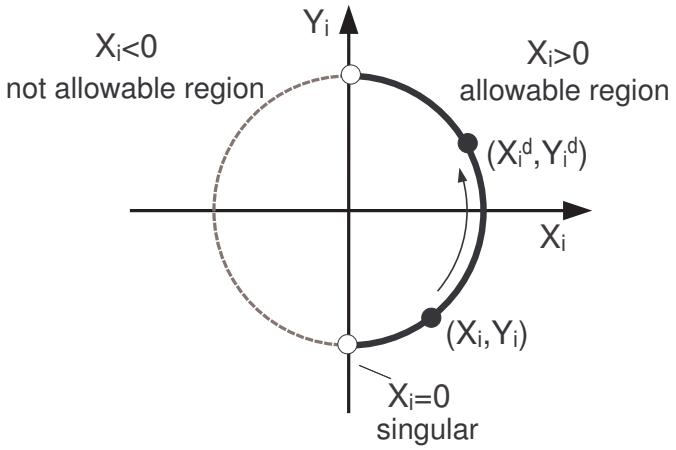

FIGURE 4.3: Geometric illustration of (X_i, Y_i) and (X_i^d, Y_i^d), where $X_i > 0$ is enforced to avoid singularity of ξ_x at $X_i = 0$ in (3.3).

where $\gamma > 0$ is the control gain. Then, injecting this control (4.4) into (4.3), we have

$$\frac{d}{dt}(Y_i - Y_i^d) = -\gamma X_i (Y_i - Y_i^d) \tag{4.5}$$

where $\gamma X_i \geq \gamma\mu =: \gamma'$, where $\mu > 0$ is defined s.t. $X_i(t) \geq \mu > 0$, implying that $Y_i(t) \to Y_i^d$ exponentially at least with the convergence rate of $\gamma' > 0$. The relation (4.5) also implies that there will indeed no overshoot for Y_i, thereby, guarantees that (X_i, Y_i) always stays within the first and fourth quadrants of Fig. 4.3.

If $Y_i(t)$ is close enough to Y_i^d (i.e., if $|Y_i(t) - Y_i^d| \leq \epsilon_1$ for a small $\epsilon_1 > 0$), we then turn off the control u_i^r. Then, with $u_i^r = 0$ and $u_x = 1$, we have

$$\dot{X}_i = \dot{Y}_i = 0$$

(i.e., $\dot{\alpha}_i = \dot{\beta}_i = 0$). Moreover, with $u_x = 1$, we have $\phi_i \to 0$ according to the stabilizing dynamics of (4.2), thus, completing the final stage of the sequence in Fig. 4.2.

4.1.3 Avoidance Feasibility

An immediate question would then be whether it is possible to complete the avoidance sequences in Fig. 4.2 before collision with the obstacle. To determine this *feasibility condition of reconfiguration*, given the shapes of the robots/obstacles and the distances among them, we first (conservatively) estimate the collision time T_c, at which one of the robots or the grasped object can collide with the obstacle. This can be determined by shortest distance between robots/object and obstacles because its velocity is fixed as $(u_x, u_y) = (1, 0)$. We also denote the time durations in Fig. 4.2 for the initial condition to second configuration by T_1 (i.e., $|Y_i(T_1 + T_0) - Y_i^d| \leq \epsilon_1$), and the next stage by T_2 (i.e., $|\phi_i(T_2 + T_1 + T_0)| \leq \epsilon_2$), where $\epsilon_1, \epsilon_2 > 0$ are some small numbers. Then, we can say that the reconfiguration avoidance strategy of Fig. 4.2 is feasible if

$$T_1 + T_2 \leq T_c$$

with $(u_x, u_y) = (1, 0)$ and $\phi_i(T_0) = 0$.

However, It is difficult to determine the exact T_1, T_2 *a priori*. Thus, we instead utilize their (conservative) estimates to predict the reconfiguration feasibility. For this, we can first estimate an upper-bound $\bar{T}_1$ for T_1, since, during this stage, $Y_i \to Y_i^d$ exponentially at least with the convergence rate of γ', where $\min X_i$ can be estimated from Fig.4.3. From (4.5), $\bar{T}_1$ is $|Y_i(\bar{T}_1 + T_0) - Y_i^d| \leq |(Y_i(T_0) - Y_i^d)e^{-\gamma' \bar{T}_1}| = \epsilon_1$. For the second stage, we would be able to estimate an upper-bound $\bar{T}_2$ for T_2, if $\phi_i(T_1 + T_0)$ were known, according to (4.2).

Yet, this $\phi_i(T_1 + T_0)$ is difficult to estimate, since, the evolution of ϕ_i is coupled with both $u_i^r \xi_i^r$ and $u_x \xi^x$ during T_1 interval s.t.,

$$\dot{\phi}_i = u_i^r - \frac{1}{X_i} \sin \phi_i = \gamma(Y_i - Y_i^d) - \frac{1}{X_i} \sin \phi_i \tag{4.6}$$

where u_i^r is given in (4.4) and $X_i > 0$ as shown after (4.5). Instead of this $\phi_i(T_1 + T_0)$, we then utilize an upper bound $\bar{\phi}_i(T_1 + T_0)$ to estimate $\bar{T}_2$ as defined by

$$\dot{\bar{\phi}}_i := u_i^r = \gamma(Y_i - Y_i^d) \tag{4.7}$$

with $\bar{\phi}_i(T_0) = 0$. We can then show that

$$|\bar{\phi}_i(T_1 + T_0)| \geq |\phi_i(T_1 + T_0)|$$

since: 1) $(Y_i(t) - Y_i^d) \cdot \bar{\phi}_i(t) \geq 0 \; \forall t \in [T_0, T_0 + T_1]$, since $Y_i \to Y_i^d$ exponentially with no overshoot; 2) from (4.6), $\gamma(Y_i - Y_i^d)$ drives ϕ_i only along one direction (since the sign of $Y_i - Y_i^d$ does not change) with

$$\begin{aligned} \left| \int_{T_0}^{T_1+T_0} \gamma(Y_i - Y_i^d) dt \right| &= \left| \int_{T_0}^{T_1+T_0} u_i^r dt \right| \\ &= |\alpha_i(T_1 + T_0) - \alpha_i(T_0)| < \pi \end{aligned}$$

if not, X_i should change its sign as can be seen from Fig. 4.3, thus, 3) the term $-\frac{1}{X_i} \sin \phi_i$ in (4.6) will oppose against this input $\gamma(Y_i - Y_i^d)$ for all $t \leq T_1 + T_0$ (since $|\int_{T_0}^{T_1+T_1} u_i^r dt| < \pi$, under which $\phi_i \cdot \sin \phi_i \geq 0$), thereby, reducing the change in ϕ_i. Moreover, we can obtain this upper bound $\bar{\phi}_i(T_1 + T_0)$ simply by solving

$$|Y_i(\alpha_i(T_0) - \bar{\phi}_i(T_1 + T_0)) - Y_i^d| = \epsilon_1$$

since we have, from (4.7) with $\dot{\alpha}_i = -u_i^r$, $\bar{\phi}_i(T_1+T_0) = \bar{\phi}(T_0) - \alpha_i(T_1+T_0) + \alpha_i(T_0)$ with $\bar{\phi}_i(T_0) = \phi_i(T_0) = 0$ and also, during the first stage of Fig. 4.2, Y_i only depends on α_i (with $\dot{\beta}_i = 0$). See Fig. 4.4 and Fig. 2.1(b).

On the other hand, during the second stage, the platform angle $\phi_i \to 0$ from $\phi_i(T_1 + T_0)$ according to (4.2). Using $\bar{\phi}_i(T_1 + T_0)$ computed as above, we can then estimate $\bar{T}_2$ by using the following dynamics (rather than (4.2)):

$$\dot{\bar{\phi}}_i = -\eta \bar{\phi}_i \tag{4.8}$$

where $\eta > 0$ is chosen s.t. $|\frac{1}{X_i} \sin \bar{\phi}_i| \geq |\eta \bar{\phi}_i|$ for all $|\bar{\phi}_i| \leq |\bar{\phi}_i(T_1 + T_0)|$. Such

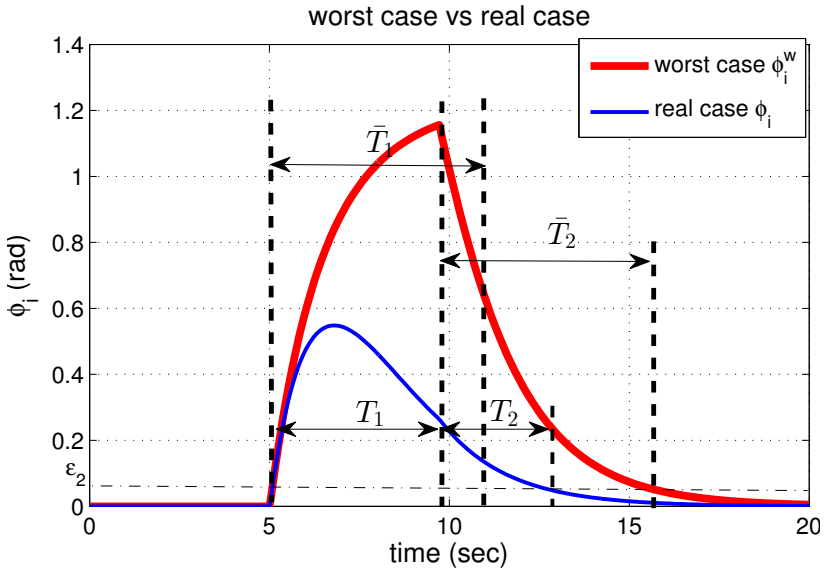

FIGURE 4.4: Examples of upper bound $\bar{\phi}_i(t)$ and real $\phi_i(t)$ during the reconfiguration sequence in Fig. 4.2 with $Y_i^d < Y_i$. Note that $\bar{T}_1 \geq T_1$, $\bar{T}_2 \geq T_2$ and $|\bar{\phi}_i(t)| \geq |\phi_i(t)|$. Here, $\bar{T}_1$ and $\bar{T}_2$ overlap with each other, since $\bar{T}_1$ is computed from (4.5), while $\bar{T}_2$ from (4.8) with $\bar{\phi}_i(T_1 + T_0)$ (not with $\bar{\phi}_i(\bar{T}_1 + T_0)$).

$\eta > 0$ exists since $|\bar{\phi}_i(T_1 + T_0)| = |\alpha_i(T_1 + T_0) - \alpha_i(T_0)| < \pi$ as explained before (4.7). The upper bound $\bar{T}_2$ can then be estimated by $|\bar{\phi}_i(\bar{T}_2 + T_1 + T_0)| = |\bar{\phi}_i(T_1 + T_0)e^{-\eta \bar{T}_2}| = \epsilon_2$. We can then assert that, given T_c, the reconfiguration avoidance strategy is feasible if $\bar{T}_1 + \bar{T}_2 \leq T_c$. See Fig. 4.4.

Fig. 4.1(c) present snapshots of this reconfiguration-based obstacle avoidance, where the mobile manipulators together reconfigure their formation to avoid the obstacle while keeping the intended trajectories (i.e., $u_x = 1$) of their end-effectors and the grasped object and also rigidly maintaining the grasping shape

with no grasping-enforcing fixture.

Chapter 5

Conclusion and Future Work

5.1 Conclusion

In this thesis, we propose a novel control framework for fixture-less cooperative grasping and obstacle avoidance for multiple planar kinematic mobile manipulators under nonholonomic constraints. Using the nonholonomic passive decomposition [1], we can divide the system's behaviors into: 1) grasping aspect; 2) grasped object maneuver; and 3) internal motions. Then, by controlling these aspects separately and simultaneously while also utilizing some peculiar dynamics of the internal motions, we can allow the robots to drive the grasped object according to velocity commands, while rigidly maintaining the grasping shape

with no dedicated contact/grasp-enforcing fixture and also avoiding obstacles either by whole formation maneuver (for large obstacle) or by internal formation reconfiguration (for small obstacle). Simulation results are also presented.

5.2 Future Work

From proposed results, some possible future research topics include: 1) extension to 3D tasks and dynamic mobile manipulators; and 2) real implementation. This paper consider planar mobile manipulator, however, 3D mobile manipulator that have more DOF can achieve more useful tasks in real environment. Obstacle is also three dimensional object actually, then extension to 3D tasks provide more rich motion and can be used to realistic application. Also, we address kinematic control in this paper, then consideration of dynamic mobile manipulator will achieve more precise control. Only simulation is presented here. Real implementation should be done in the future to verify usefulness of our method and there will be exists other issue such as stability.

Bibliography

[1] D. J. Lee. Passive decomposition and control of nonholonomic mechanical systems. *IEEE Transactions on Robotics*, 26(6):978–992, 2010.

[2] D. J. Lee. Passive decomposition of multiple nonholonomic mechanical systems under motion coordination requirements. In *Proc. IFAC World Congress*, 2008.

[3] Y. Yamamoto and X. Yun. Coordinating locomotion and manipulation of a mobile manipulator. *IEEE Transactions on Automatic Control*, 39(6): 1326–1332, 1994.

[4] H. Seraji. A unified approach to motion control of mobile manipulators. *International Journal of Robotics Research*, 17(2):107–118, 1998.

[5] P. G. Dauchez, editor. *Journal of Robotic Systems: Special Issue on Mobile Manipulators*, volume 13. November 1996.

[6] O. Brock and C. C. Kemp editors. *Autonomous Robots: Special Issue on Autonomous Mobile Manipulation Manipulators*, 28, November 2010.

[7] O. Khatib, K. Yokoi, K. Chang, D. Ruspini, R. Holmberg, and A. Casal. Coordination and decentralized cooperation of multiple mobile manipulators. *Journal of Robotic Systems*, 13(11):755–764, 1996.

[8] H. G. Tanner, S. G. Loizou, and K. J. Kyriakopoulos. Nonholonomic navigation and control of cooperating mobile manipulators. *IEEE Transactions on Robotics & Automation*, 19(1):53–64, 2003.

[9] D. J. Lee. Semi-autonomous teleoperation of multiple wheeled mobile robots over the internet. In *Proc. ASME Dynamic Systems & Control Conference*, pages 147–154, 2008.

[10] D. J. Lee and M. W. Spong. Bilateral teleoperation of multiple cooperative robots over delayed communication networks: Theory. In *Proc. IEEE Int'l Conference on Robotics and Automation*, pages 360–365, 2005.

[11] J. P. Desai, J. P. Ostrowski, and V. Kumar. Modeling and control of formations of nonholonomic mobile robots. *IEEE Transactions on Robotics and Automation*, 17(6):905–908, 2001.

[12] P. Tabuada, G.J. Pappas, and P. Lima. Motion feasibility of multi-agent formations. *IEEE Transactions on Robotics*, 21(3):387–392, 2005.

[13] D. J. Lee and P. Y. Li. Passive decomposition of mechanical systems with coordination requirement. *IEEE Transactions on Automatic Control*, 58(1): 230–235, 2013.

[14] Y. Hirata, Y. Kume, Zhi-Dong Wang, and K. Kosuge. Handling of a single object by multiple mobile manipulators in cooperation with human based on virtual 3-d caster dynamics. *JSME International Journal Series C Mechanical Systems, Machine Elements and Manufacturing*, 48(4):613–619, 2005.

[15] C. P. Tang, R. M. Bhatt, M. Abou-Samah, and V. Krovi. Screw-theoretic analysis framework for cooperative payload transport by mobile manipulator collectives. *IEEE/ASME Transactions on Mechatronics*, 11(2):169–178, 2006.

[16] T.G. Sugar and V. Kumar. Control of cooperating mobile manipulators. *IEEE Transactions on Robotics and Automation*, 18(1):94–103, 2002.

[17] R. Holmberg and O. Khatib. Development and control of a holonomic mobile robot for mobile manipulator tasks. *International Journal of Robotics Research*, 19(11):1066–1074, 2000.

[18] M. W. Spong, S. Htchinson, and M. Vidyasagar. *Robot modeling and control.* WILEY, 2006.

[19] R. M. Murray, Z. Li, and S. S. Sastry. *A mathematical introduction to robotic manipulation.* CRC, Boca Ranton, FL, 1993.

[20] X. Yun and Y. Yamamoto. Stability analysis of the internal dynamics of a wheeled mobile robot. *Jounal of Robotic Systems*, 14(10):697–709, 1997.

요 약

본 논문에서는 다중이동조작 로봇의 새로운 기구학적 협업제어 기법에 대해서 기술한다. 제안된 제어기법을 통해 이동조작 로봇이 협업하여 움켜쥔 물체를 원하는 속도로 이동시킬 수 있으며, 동시에 물체를 움켜진 대형을 유지시켜주는 구조물 없이 대형을 유지시키며 이동하며, 뿐만아니라 전체적인 경로를 변화시키거나 여자유도를 이용한 내부적인 움직임을 이용하여 장애물을 회피하는 등의 임무 수행이 가능하다. 이러한 제어기법을 제안하기 위해 nonholonomic passive decomposition기법을 [1, 2] 이용하여 로봇의 움직임을 세가지 측면으로 분류하여 고려하였다. (각각은 움켜쥔 형태, 움켜쥔 물체의 이동, 내부 움직임이 있음) 이 기법을 통해 각각의 움직임을 동시에 그리고 분리하여 제어할 수 있게 되었다. 또한 내부 움직임의 독특한 특성을 이용하여 물체의 경로를 변경하지 않고도 장애물을 회피할 수 있는 기법을 제안하였다. 마지막으로 제안된 방법을 이용한 시뮬레이션 결과를 제시한다.

주요어: Nonholonomic constraint, Mobile manipulator, Obstacle avoidance, Cooperative control

학번: *2012-20681*

Acknowledgements

First of all, I would like to express my special appreciation and thanks to my advisor, Professor. Dongjun Lee. Without his guidance and sincere advice throughout my time for Master Science degree this thesis would not have been possible. Thanks to his guidance, I have learned delight of research.

I would also like to express my gratitude to all members of the Interactive & Networked Robotics Lab. who have helped me over the past two years; Changsu Ha, Youngsun Nam, Myungsin Kim, Nguyen Hai Nguyen, Hyunjun Cho, Francis Byonghwa Choi, Inyoung Jang, Sangyul Park, Jinhoo Lee, Jaemin Yun and Yongseok Lee.

I have had the support and encouragement of my parents and older sister over the years. I would like to thank my family, for supporting me spiritually throughout my like.

This thesis is based upon work supported by the Basic Science Research Program (2012- R1A2A2A0-1015797) of the National Research Foundation (NRF) of Korea funded by the Ministry of Education, Science & Technology (MEST)